# Observation of a large $\beta$-delayed neutron emission component in $^{102}$Rb decay and identification of excited states in $^{102}$Sr

Z. M. Wang,[1,2] A. B. Garnsworthy,[1,*] C. Andreoiu,[2] G. C. Ball,[1] P. C. Bender,[1,†] V. Bildstein,[3] D. S. Cross,[2] G. Demand,[3] R. Dunlop,[3] L. J. Evitts,[1] P. E. Garrett,[3] G. Hackman,[1] B. Hadinia,[3] S. Ketelhut,[1] R. Krücken,[1,4] K. G. Leach,[3,‡] A. T. Laffoley,[3] D. Miller,[1,§] M. Moukaddam,[1] J. Pore,[2] A. J. Radich,[3] M. M. Rajabali,[1,‖] C. E. Svensson,[3] A. Tan,[3] E. Tardiff,[1,¶] C. Unsworth,[1,**] A. Voss,[1,5,††] and P. Voss[2,‡‡]

[1]*TRIUMF, 4004 Wesbrook Mall, Vancouver, British Columbia, Canada V6T 2A3*

[2]*Department of Chemistry, Simon Fraser University, Burnaby, British Columbia, Canada V5A 1S6*

[3]*Department of Physics, University of Guelph, Guelph, Ontario, Canada N1G 2W1*

[4]*Department of Physics and Astronomy, University of British Columbia, Vancouver, British Columbia, Canada V6T 1Z1*

[5]*The University of Manchester, Manchester M13 9PL, United Kingdom*

(Received 20 January 2015; revised manuscript received 1 April 2016; published 2 May 2016)

The $\beta$ decay and $\beta$-delayed neutron emission of $^{102}$Rb have been studied using the $8\pi$ spectrometer at TRIUMF-ISAC. The level scheme of $^{102}$Sr has been expanded from results of a $\gamma$-$\gamma$ coincidence analysis, including the identification of the $(4^+)$ member of the ground-state band. The $\beta$-delayed neutron branching ratio of $^{102}$Rb was found to be significantly larger than previously reported. This larger value has the potential to modify the results of $r$-process calculations and motivates further measurements as well as refinements of theoretical models.

DOI: 10.1103/PhysRevC.93.054301

## I. INTRODUCTION

When the difference in mass between parent and daughter nuclear states, the $Q$ value for $\beta$ decay, is greater than the neutron-separation energy in the daughter nucleus, the process of $\beta$-delayed neutron emission becomes energetically possible. The latest atomic mass evaluation [1] includes data for ~3000 nuclei that have been studied experimentally [2], and of these, 606 nuclei have $\beta$-delayed neutron emission as an energetically allowed decay process. These ~3000 nuclei studied to date are only a fraction of the ~7000 nuclei predicted to be particle bound by modern density functional theory [3]. It is expected that $\beta$-delayed neutron emission will be the dominant decay process for the majority of these as yet undiscovered nuclei. When $\beta$-delayed neutron emission is energetically possible there is a competition between $\beta$ decay to states above and below the neutron separation energy in the daughter nucleus that is reflected in the $\beta$-delayed neutron emission branching ratio of the parent nucleus. This decay process is of particular importance for understanding the observed elemental abundances resulting from the astrophysical rapid neutron capture, the $r$-process, responsible for contributing approximately half of the observed abundance of the heavy elements in our universe [4,5]. It is also well established that detailed knowledge of the neutrons released in the $\beta$-delayed neutron emission decay of fission products plays a key role in the operation of nuclear reactors [6] and in the management of spent nuclear fuel through decay-heat generation [7].

Because the neutron-rich isotope $^{102}$Rb lies close to the region of $r$-process nucleosynthesis [4,5], its decay properties are of interest as input to $r$-process calculations. In addition to mass, half-life ($T_{1/2}$), of the ground state and $\beta$-delayed neutron emission probability ($P_n$) are fundamental in determining the $r$-process flow and final element abundances [4,5,8]. It has been shown that there is a particular sensitivity to these properties in "cold" $r$-process scenarios during the decay to stable isotopes at the later stages of the process and following freeze-out [9,10].

The first reported $T_{1/2}$ and $P_n$ measurements for $^{102}$Rb of 37(5) ms and 18(8)%, respectively, were reported by Pfeiffer *et al.* [11] in studies of a mass-separated source produced from proton-induced fission of natural uranium. The most recent $T_{1/2}$ measurements are $35(\pm^{15}_{8})$ [12] and 37(10) ms [13] in which $^{102}$Rb was produced and identified ion-by-ion from the fragmentation of a $^{238}$U beam.

The first excited state of the daughter nucleus, $^{102}$Sr, was observed in a $\beta$-decay study [14]. The 126-keV $2^+$ state was assigned based on the energy systematics and lifetime of the measured adjacent even-$A$ strontium isotopes, i.e., $^{98}$Sr and $^{100}$Sr. The corresponding $2^+$ level half-life of 3.0(12) ns corresponds to an $E2$ transition with an enhancement of approximately 100 Weisskopf units.

In this article we report new experimental results that extend the level scheme of $^{102}$Sr and a new measurement of

*garns@triumf.ca

†Present address: National Superconducting Cyclotron Laboratory, Michigan State University, East Lansing, MI 48824, USA.

‡Present address: Department of Physics, Colorado School of Mines, Golden, CO 80401, USA.

§Present address: Idaho National Laboratory, Idaho Falls, ID 83415, USA.

‖Present address: Department of Physics, Tennessee Technological University, Cookeville, TN 38505, USA.

¶Present address: Department of Physics, Harvard University, Cambridge, MA 02138, USA.

**Present address: Oliver Lodge Laboratory, University of Liverpool, Liverpool L69 7ZE, United Kingdom.

††Present address: University of Jyväskylä, FI-40014 Jyväskylä, Finland.

‡‡Present address: Department of Physics, Concordia College, Moorhead, MN 56562, USA.

 

the $\beta$-delayed neutron emission branching ratio. The revised value is larger than the previously reported value and has the potential to modify $r$-process flow, thus motivating additional measurements and a full evaluation of the impact of $\beta$-delayed neutron emission probabilities in this region on the $r$-process.

## II. EXPERIMENT

The isotope $^{102}$Rb was produced by reactions of a 500-MeV, 9.7-$\mu$A proton beam impinging on a multilayered $UC_x$ target at the TRIUMF-ISAC facility [15]. The Rb nuclei were surface ionized, extracted from the target, and mass-separated before being delivered to the Mylar tape at the center of the $8\pi$ spectrometer [16] at a beam energy of 26 keV and a rate of ~6.5 particles/s. The 20 Compton-suppressed high-purity germanium (HPGe) $\gamma$-ray detectors of the $8\pi$ spectrometer surrounded the vacuum chamber that housed SCEPTAR, one half hemisphere of ten plastic scintillators for $\beta$ tagging, and a single fast-timing-response plastic scintillator located at 0° to the beam axis. A trigger condition accepting singles events from all detectors was used and were synchronized by a time stamp provided by a temperature-stabilized 10-MHz clock as well as an individual time-to-digital converter (TDC) signal for each detector. Two modes of tape-movement were used during the data collection. The first mode was a continuous beam deposit on the tape that was continuously moving at a slow speed (~26 cm/s). The slow movement of the tape ensured that most of the $^{102}$Rb decays occurred within the focal volume of the $8\pi$ HPGe detectors, while the longer-lived daughter products did not. This mode maximized the statistics for the construction of a $\gamma$-$\gamma$ coincidence matrix. The second mode utilized tape cycling that had a tape movement at the beginning of the cycle and a collection of 1 s of background data, followed by the collection of data from 10 s of beam deposit and 2 s of decay with beam off. This enabled the establishment of $\gamma$-ray intensities and a measurement of the decay half-life. The HPGe detectors were calibrated for energy and efficiency using standard $\gamma$-ray sources of $^{133}$Ba, $^{152}$Eu, and $^{56}$Co. Experimental data were accumulated over a period of approximately 60 h.

At the beginning of the experiment, the mass separator was optimized for the adjacent isotope, $^{100}$Rb (~500 pps), to maximize the Rb fraction over the other components in the cocktail beam (surface-ionized $^{100}$Sr and $^{100}$Y). An extrapolation of the magnetic field value was then made to reach $^{102}$Rb. During the mass $A = 102$ implantation, the beam composition was monitored by using the relative $\gamma$-ray intensities of the 243.8-, 151.8-, and 599.6-keV $\gamma$ rays, which follow the decay of $^{102}$Sr, $^{102}$Y, and $^{102}$Zr, respectively. The presence of $^{102}$Rb in the beam was confirmed by observation of previously reported (from direct $\beta$ decay of $^{101}$Rb [17]) mutually coincident 271.0 and 92.8 keV, as well as the 111.8- and 251.4-keV $\gamma$ rays in the $\beta$-delayed neutron emission daughter nucleus, $^{101}$Sr.

## III. RESULTS AND DISCUSSION

In the present work, around 1500 counts were accumulated in $\gamma$-ray singles in the peak of the 126.1-keV transition in $^{102}$Sr in continuous-tape-movement mode, and around 5000 counts were obtained in the same peak in cycling mode. The low statistics of this $\gamma$ ray in the time period immediately following a beam-on to beam-off transition, and the relatively high contribution from other decaying species, prevented the extraction of a half-life for the $^{102}$Rb parent nucleus. This can be especially difficult for short-lived decays. However, the ratio of $\gamma$-ray intensities between continuous and cycling modes reflects the half-life. A larger ratio indicates a shorter half-life as the continuous tape movement enhances the short-lived decay components in the $\gamma$-ray spectrum by removing longer-lived species from the sight of the detectors. Typical ratios for decays from $^{102}$Sr [$T_{1/2} = 69(6)$ ms] were ~0.15 while longer-lived species had much smaller ratios [$^{102}$Zr, $T_{1/2} = 2.9(2)$ s had a ratio of 0.005]. The ratio for decays from $^{102}$Rb [$T_{1/2} = 37(5)$ ms] was ~0.3 both for $\gamma$ rays associated with the $\beta$-decay daughter, $^{102}$Sr, and the $\beta$-delayed neutron emission daughter, $^{101}$Sr. In this way, the 126.1-keV $\gamma$ ray was positively confirmed to follow the decay from $^{102}$Rb to $^{102}$Sr. The similar ratios aided the confirmation of the new $\gamma$-ray assignments discussed here from the $\gamma$-$\gamma$ coincidence analysis.

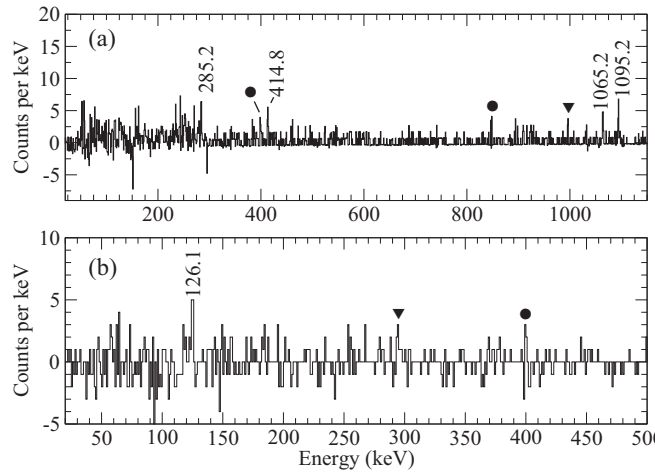


FIG. 1. (a) Portion of the $\gamma$-ray energy spectrum in coincidence with the 126.1-keV transition in $^{102}$Sr. (b) The $\gamma$-ray energy spectrum gated on the 285.2-keV transition in $^{102}$Sr. Both spectra require a coincidence with a $\beta$ particle and are random-background subtracted. Peaks from other decay species are indicated by the following symbols: ▼ for $^{101}$Sr–$^{101}$Y and • for $^{102}$Nb–$^{102}$Mo.

Energy-gated $\gamma$-ray spectra measured in coincidence with $\beta$ particles are presented in Fig. 1 and the experimentally determined level scheme of $^{102}$Sr from the $\beta$ decay of $^{102}$Rb is presented in Fig. 2. The 285.2-keV $\gamma$ ray has been assigned tentatively as the $(4^+)$ to $(2^+)$ transition in $^{102}$Sr on the basis of $\gamma$-$\gamma$ mutual energy coincidence and the systematic trend of the energies of the $4^+$ states in adjacent neutron-rich $^{98,100}$Sr isotopes.

The level energy ratio of the tentatively assigned excited states $E(4^+)/E(2^+) = 3.26$ approaches the collective rotor limit of 3.33. The ground-state band structure of $^{102}$Sr appears nearly identical to that observed in the neighboring $^{98}$Sr and $^{100}$Sr nuclei indicating that the well-deformed rotational nature of the neutron-rich Sr isotopes continues towards the $N = 66$ neutron midshell.

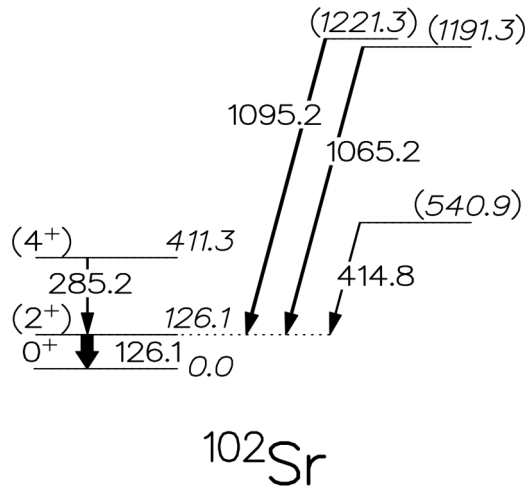


FIG. 2. Proposed $^{102}$Sr level scheme from the present $^{102}$Rb $\beta$-decay experiment. The width of the arrows represents their relative intensity. The placements in the level scheme are based on mutual $\gamma$-$\gamma$ energy coincidences. The systematic comparison suggests a tentative $(4^+)$ state at an energy of 411.3 keV.

Table I presents the parent level energy, the transition energy, and the relative intensities populated in the $\beta$ decay of $^{102}$Rb to $^{102}$Sr as measured in the present work. The $\beta$-decay branching ratios to the different levels are not given because of the unknown contribution of direct feeding to the ground state. As well as confirmation of the previously reported 126.1-keV $\gamma$ ray, these new data allow the transitions of 285.2, 414.8, 1065.2, and 1095.2 keV to be assigned to $^{102}$Sr. The reported transition intensities are made following correction for internal conversion.

If one examines the energy systematics of the $6^+$ to $4^+$ transition in the neighboring even-even Sr nuclei, then one can consider placing the 414.8-keV transition as feeding the 411.3-keV state. However the observed $\gamma$-ray intensities do not support such a placement. The coincidence data indicate that the 414.8-keV transition is in mutual coincidence with the 126.1-keV transition only, and no coincidence between the 285.2- and 414.8-keV $\gamma$ rays is observed in the present study [see Fig. 1(b)]. In addition, because the observed intensity of the 285.2- and 414.8-keV transitions is similar to that in the gate on the 126.1-keV transition [Fig. 1(a)], a placement as the $6^+$ to $4^+$ transition would imply significant feeding to the $6^+$ state in $\beta$ decay and essentially no feeding to the $4^+$ state. As is discussed later, our data favors the suggested $4^+$ spin assignment for the parent state in $^{102}$Rb, which is unlikely to preferentially populate the $6^+$ state in $^{102}$Sr. Therefore this 414.8-keV $\gamma$ ray is placed as feeding the 126.1-keV state from an excited state at 540.9 keV. Any deexcitation directly to the ground state from this state could not be identified or ruled out in the present work.

This state at 540.9 keV would be a candidate for the second $0^+$ state or the second $2^+$ state. A spin and parity of $0^+$ seems unlikely because the energy of the second $0^+$ state is increasing in energy (i.e., 215 and 938 keV in $^{98,100}$Sr, respectively) as one moves away from the change in ground-state configuration that occurs at $N = 58 \rightarrow 60$. Other $J^\pi$ values are unlikely at such low energy in a nucleus displaying appreciable deformation in the ground state. Such a state at 540.9 keV could therefore represent the second $2^+$ state in $^{102}$Sr, leading to an energy ratio of the second to first $2^+$ states of $R_{22} = 4.29$. However, this value of the $R_{22}$ is substantially lower than a typical value seen in the rare-earth region [18] for equivalent $R_{42}$ values and makes such a spin assignment also questionable. Therefore no spin assignment is suggested for the 540.9-keV state in the present work.

Figure 3 shows the $\gamma$-ray mutual coincidences found in $^{101}$Sr. The $^{101}$Sr level scheme deduced from the $^{102}$Rb $\beta$-delayed neutron emission data in the current work is shown in Fig. 4. The level scheme is in agreement with that reported by

TABLE I. Level and transition properties of $^{101}$Sr and $^{102}$Sr populated in the decay of $^{102}$Rb. The $\gamma$-ray intensities in $^{101}$Sr are normalized to that of the 271.0-keV transition after correction for internal conversion. Transition intensities in $^{102}$Sr are separately normalized to that of the 126.1-keV transition after correction for internal conversion.

| $^{101}$Sr | | | $^{102}$Sr | | |
|---|---|---|---|---|---|
| $E_{level}$ (keV) | $E_\gamma$ (keV) | $I$ | $E_{level}$ (keV) | $E_\gamma$ (keV) | $I$ |
| 111.8(2) | 111.8(2) | 36.8(25) | 126.1(2) | 126.1(2) | 100.0(54) |
| 257.3(3) | 145.5(2) | 4.9(12) | 411.3(3) | 285.2(2) | 14.1(41) |
| 271.0(2) | 271.0(2) | 100.0(29) | 540.9(3) | 414.8(2) | 11.7(21) |
| 363.1(2) | (92.1)(3) | 2.0(5) | 1191.3(3) | 1065.2(2) | 26.0(51) |
| 363.1(2) | 251.4(2) | 25.3(60) | 1221.3(3) | 1095.2(2) | 28.9(55) |
| 363.1(2) | 363.1(2) | 10.5(15) | | | |
| 363.8(3) | 92.8(2) | 37.0(26) | | | |
| 405.8(3) | 134.8(2) | 18.9(23) | | | |
| 489.6(4) | 232.3(2) | 3.2(16) | | | |
| 523.0(3) | 160.8(2) | 10.3(23) | | | |

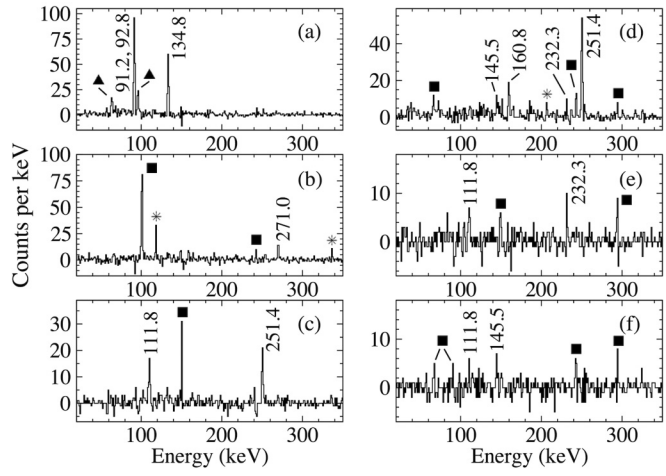


FIG. 3. Coincidence-energy-gated and random-background-subtracted $\gamma$-ray spectra in coincidence with a $\beta$ particle, gated on the (a) 271.0-, (b) 134.8-, (c) 160.8-, (d) 111.8-, (e) 145.5-, and (f) 232.3-keV transitions in $^{101}$Sr. Peaks from other decay species are indicated by the following symbols: ▲ for $^{102}$Zr–$^{102}$Nb, ■ for $^{102}$Sr–$^{102}$Y, and ∗ for $^{101}$Zr–$^{101}$Nb.

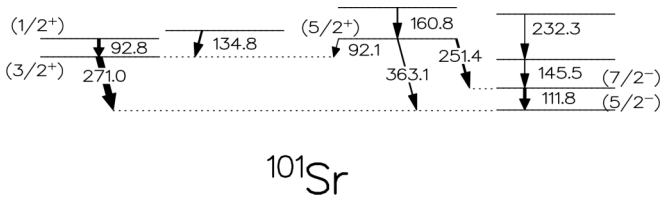


FIG. 4. Proposed $^{101}$Sr level scheme following $^{102}$Rb $\beta$-delayed neutron emission. The width of the transitions represent their relative intensities. The transition assignments are based on mutual coincidence in a $\gamma$-$\gamma$ analysis. The tentative $J^\pi$ assignments are from Ref. [17].

Lhersonneau *et al.* [17] with the exception of a relocation of the 232.3-keV transition and the addition of the 134.8-, 145.5-, and 160.8-keV transitions from a $\gamma$-$\gamma$ coincidence analysis in the present work. Mutual coincidences have been observed between all transitions shown in the $^{101}$Sr level scheme except the 271.0- and 92.1-keV transitions due to the overlap with the more intense 92.8-keV line. In general the low-lying excited states populated in $^{101}$Sr following the $\beta$-delayed neutron emission process were the same as those observed in the direct $\beta$ decay of $^{101}$Rb [17]. However the relative intensities were very different. In addition, the 1362.9-keV level that was strongly populated in $\beta$ decay was not observed in the $\beta$-delayed neutron emission. The $\gamma$-ray energies and relative intensities as well as the parent level information from the present work are shown in Table I.

Pfeiffer *et al.* [11] suggested that the last proton in the neutron-rich rubidium isotopes occupies the 3/2[431] Nilsson orbital while neutrons are filling a series of different orbitals (see, for example, Fig. 6 of Ref. [19] for the Nilsson orbitals in this region). The $J^\pi$ value of the $^{101}$Rb ground state is assigned to be $3/2^+$ from a proton in the 3/2[431] orbital as was discussed by Lhersonneau *et al.* [17]. Also suggested by Lhersonneau *et al.* [17], the ground-state $J^\pi$ value in $^{101}$Sr is likely to be $(5/2^-)$ formed when the odd neutron occupies the $\nu$5/2[532] orbital. The increase of quadrupole deformation seen in $^{98}$Sr, $^{100}$Sr, and $^{102}$Sr also suggests that the last pair of neutrons occupy the 5/2[532] orbital in $^{102}$Sr [20]. Consequently, the last neutron in $^{102}$Rb would occupy a single-particle orbital above 5/2[532]. The 5/2[413] configuration is one candidate for the valence neutron to couple with the last proton in the 3/2[431] orbital, which leads to possible $K^\pi$ values for the $^{102}$Rb ground state of $1^+$ or $4^+$ with the Gallagher-Moszkowski splitting [21] favoring the antiparallel spin coupling, or $K^\pi = 1^+$, as forming the ground state. As is indicated by the sum of the intensities feeding into the 126.1-keV state, 98.3 compared to 100.0, there is in fact virtually no direct feeding to this state. A higher spin such as the maximally aligned $4^+$ is therefore favored in the present study.

The $P_n$ value was also extracted from a comparison of the relative $\gamma$-ray yield from the $\beta$ decay and $\beta$-delayed neutron emission daughter nuclei, $^{102}$Sr and $^{101}$Sr. Only the most intense $\gamma$ rays in the daughter nuclei, which are free of background contamination, were used in this comparison. The intensities were corrected for $\gamma$-ray efficiency and internal conversion[1] using coefficients provided by BrIcc [22]. The number of counts for the 126.1-, 111.8-, and 271.0-keV $\gamma$ rays following these corrections are 8945(257), 4184(252), and 11115(238), respectively. The intensity must also be corrected for the relative branching ratio of the transition. Uncertainty exists in the intensity of the direct decay branch to the ground state of both $^{101}$Sr and $^{102}$Sr. This direct feeding is difficult to measure in the present study due to the many contributions to the $\beta$ spectrum. Table II shows the experimental values for the absolute intensity of the $2_1^+$ to $0^+$ transition in the $\beta$ decay of the neutron-rich, even-mass Rb isotopes and Table III shows the experimental values for the direct ground-state feeding in $\beta$-delayed neutron emission of the same parent nuclei. Based on this systematic information it is reasonable to set a limit on the absolute intensity of the $2_1^+$ to $0^+$ transition following the $\beta$ decay of $^{102}$Rb to be between 50% and 80%, as is shown in the final row of Table II. In addition, the range of values for the direct feeding to the ground state of $^{101}$Sr in $\beta$-delayed neutron emission can be constrained to between 0% and 70% (shown in the final row of Table III). These values taken from the systematics of the region will be used to set limits on the $\beta$-delayed neutron branching ratio in the present measurement.

TABLE II. Systematics of the experimental values [23] for the absolute intensity of the $2_1^+$ to $0^+$ transition in the $\beta$ decay of the neutron-rich, even-mass Rb isotopes. The final row indicates the range used for the $^{102}$Rb case in the present work.

| Decay | $J_i^\pi \rightarrow J_f^\pi$ | $L$ | Absolute intensity of $2_1^+$ to $0^+$ transition |
|---|---|---|---|
| $^{94}$Rb–$^{94}$Sr | $3^-$–$2^+$ | 1 | 61(4)% |
| $^{96}$Rb–$^{96}$Sr | $2^{(-)}$–$2^+$ | 0 | 78(2)% |
| $^{98}$Rb–$^{98}$Sr | $(0,1)$–$2^+$ | (1,2) | ∼46% |
| $^{98}$Rb$^m$–$^{98}$Sr | $(3,4)$–$2^+$ | (1,2) | 69(2)% |
| $^{100}$Rb–$^{100}$Sr | $(3^+,4^+)$–$2^+$ | 2 | 55(1)% |
| $^{102}$Rb–$^{102}$Sr | $(4^+)$–$2^+$ | 2 | 50%–80% |

If one assumes the branching to the ground state of $^{101}$Sr to be zero and the intensity of the $2^+$ to $0^+$ transition in $^{102}$Sr to be 50%, a value of 46(3)% for $P_n$ is determined. This is a lower limit in the present work and assumes that all the feeding to excited states in $^{101}$Sr results in the emission of either the 111.8-keV $\gamma$ ray or the 271.0-keV $\gamma$ ray and that 50% of decays to $^{102}$Sr feed through the $2^+$ to $0^+$ transition. This value will increase if there exists any direct feeding to either the ground state of $^{101}$Sr or to excited states decaying by unobserved $\gamma$-ray cascades.

Allowing up to 70% direct feeding to the ground state of $^{101}$Sr, rather than zero, and assuming 80% of decays result in a 126.1-keV $\gamma$ ray from $^{102}$Sr, leads to a $\beta$-delayed neutron emission branching ratio of 81(6)%. We therefore adopt a

[1]Here the 126.1-keV $\gamma$ ray was assumed to be a pure $E2$ transition and the 271-keV transition a purely $E1$ transition. For the mixing ratios of the 111.8- and 271.0-keV transitions in $^{101}$Sr we have assumed the same values as those used in Ref. [14].

TABLE III. Systematics of the experimental values [23] for the direct ground-state feeding in $\beta$-delayed neutron emission of the neutron-rich, even-mass Rb isotopes. The final row indicates the range used for the $^{102}$Rb case in the present work.

| Decay | $J_i^\pi \rightarrow J_f^\pi$ | $L$ | Branching ratio to ground state |
|---|---|---|---|
| $^{94}$Rb–$^{93}$Sr | $3^-$–$5/2^+$ | 0 | 73(3)% |
| $^{96}$Rb–$^{95}$Sr | $2^{(-)}$–$1/2^+$ | 1 | 24(3)% |
| $^{98}$Rb–$^{97}$Sr | $(0,1)$–$1/2^+$ | (0) | 10(1)% |
| $^{100}$Rb–$^{99}$Sr | $4^-$–$3/2^+$ | 2 | ≈50% |
| $^{102}$Rb–$^{101}$Sr | $(4^+)$–$(5/2^+)$ | 1 | 0%–70% |

value from the present work of 65(22)%. The uncertainty is dominated by the unknown feeding to the ground states of the daughter nuclei.

As discussed in Ref. [14], although the resolution of the mass separator should prohibit transmission of $^{101}$Rb, there is a finite possibility of it being present in the delivered beam. This may have an impact on the measured $P_n$ value. An upper limit for the rate of $^{101}$Rb in the beam was determined in the present work from the nonobservation of the 1091.8-keV transition in $^{101}$Sr, which is populated in the direct $\beta$ decay of $^{101}$Rb but not in the $\beta$-delayed neutron emission of $^{102}$Rb. This upper limit was found to have a negligible effect on the measured $P_n$ value.

The $P_n$ probability for $^{102}$Rb was previously reported as 18(8)% [11], which is surprisingly small when compared with the systematic trend of adjacent neutron-rich Rb nuclei shown in Fig. 5. Here the values of $P_n/T_{1/2}$ are plotted against the $Q_{\beta n}$ value for each member of the isotopic chain as suggested by

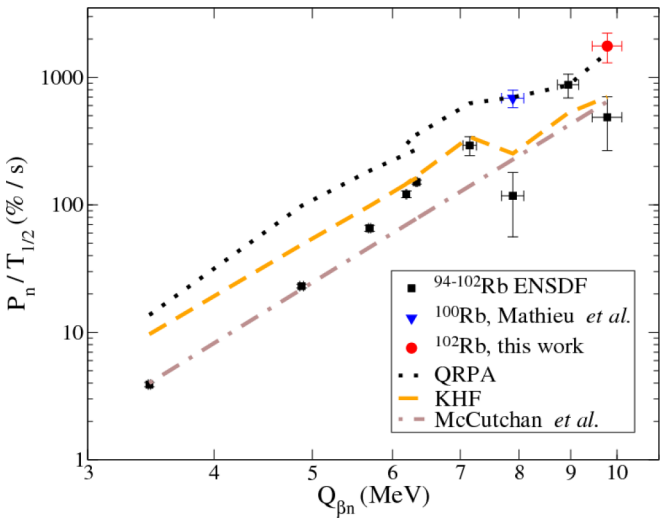


FIG. 5. The ratio of $P_n/T_{1/2}$ plotted as a function of the $Q_{\beta n}$ value for Rb isotopes. Experimental data are from Refs. [1,23]. New experimental data for $^{100}$Rb are taken from Mathieu *et al.* [26] and the $^{102}$Rb value is taken from the present work. The calculations use the QRPA [20] and KHF [27] models with values taken from Ref. [28], in addition to the prediction from Ref. [24], which is a fit to the ENSDF data [23].

McCutchan *et al.* [24]. The $Q_{\beta n}$ values are taken from Ref. [1] which includes recent measurements for $^{97,98,100}$Rb [25]. The earlier reported $P_n$ values for both $^{100}$Rb and $^{102}$Rb come from the same measurement [11], in which the results were normalized by the $P_n$ values of $^{87}$Br and $^{94,95}$Rb, and both lie below the systematic trend. A preliminary value of ∼35% for the $P_n$ of $^{100}$Rb is reported by Mathieu *et al.* [26] (no uncertainty is provided in Ref. [26] so the uncertainty shown is only from the $T_{1/2}$ and $Q_{\beta n}$ measurements). The new data point from the $8\pi$ spectrometer appears to lie close to the systematic trajectory of the lighter Rb nuclei.

These experimental values are compared to calculations of these quantities in Fig. 5. The results of three predictions are shown. The first is based on quasiparticle random-phase-approximation (QRPA) calculations [20] and the second is the empirical Kratz-Herrmann formula [27]. The predictions for both models are taken from Ref. [28]. The third calculation is the model suggested by McCutchan *et al.* [24], which is a fit to the ENSDF data [23]. All three reproduce the general trend of this isotopic chain. It is interesting how well the QRPA calculation matches the new values for the well-deformed Rb isotopes with $N > 60$.

## IV. CONCLUSION

The use of the $8\pi$ spectrometer and its associated ancillary detectors at the TRIUMF-ISAC radioactive beam facility has allowed the study of the $\beta$-decay properties of the neutron-rich nucleus $^{102}$Rb. A detailed $\gamma$-ray spectroscopic study of the $\beta$-decay daughter $^{102}$Sr and the $\beta$-delayed neutron emission decay daughter $^{101}$Sr has been performed. This has allowed the level scheme of $^{102}$Sr to be extended, including the identification of the ground-state band up to the $(4^+)$ state. The observed large relative intensity of transitions that feed the $2^+$ to $0^+$, 126-keV transition in the present work favors a $J^\pi = (4^+)$ assignment to the ground state of the $^{102}$Rb parent nucleus consistent with the assignment of the $K^\pi = 4^+$ $\nu 5/2[413] \otimes \pi 3/2[431]$ Nilsson configuration. The level energy ratio of $E(4^+)/E(2^+) = 3.26$ indicates that $^{102}$Sr is a rigid, well-deformed prolate rotor. This confirms the trend of large prolate deformation in the ground states of the $N \geqslant 60$ Sr isotopes as they approach the $N = 66$ neutron midshell.

The significantly larger $\beta$-delayed neutron emission probabilities of $^{100}$Rb and $^{102}$Rb, ∼35% [26] and 65(22)%, respectively, are in disagreement with previously reported values of 6(3)% and 18(8)%. These results may have a significant impact on the predicted flow and the $A = 99$–$102$ distribution in astrophysical $r$-process calculations. To understand these processes in more detail, the decay properties in this region need to be revisited and inconsistencies resolved using dedicated experimental setups for studying masses, $\beta$-decay properties, and the probability of $\beta$-delayed neutron emission.

## ACKNOWLEDGMENTS

The authors would like to thank the targets, beam delivery, and operations personnel at TRIUMF-ISAC for providing

the radioactive beam. This work was supported in part by the Natural Sciences and Engineering Research Council of Canada. TRIUMF receives federal funding via a contribution agreement through the National Research Council Canada. C.E.S. acknowledges support from the Canada Research Chairs program.

[1] G. Audi *et al.*, Chin. Phys. C **36**, 1287 (2012).
[2] M. Thoennessen, Rep. Prog. Phys. **67**, 1187 (2004).
[3] J. Erler *et al.*, Nature (London) **486**, 509 (2012).
[4] K. Langanke and M. Wiescher, Rep. Prog. Phys. **64**, 1657 (2001).
[5] M. Arnould, S. Goriely, and K. Takahashi, Phys. Rep. **450**, 97 (2007).
[6] G. R. Keepin, T. F. Wimett, and R. K. Zeigler, Phys. Rev. **107**, 1044 (1957).
[7] A. Tobias, Prog. Nucl. Energy **5**, 1 (1980).
[8] M. Mumpower *et al.*, Prog. Part. Nucl. Phys. **86**, 86 (2016).
[9] A. Arcones and G. Martínez-Pinedo, Phys. Rev. C **83**, 045809 (2011).
[10] M. R. Mumpower, G. C. McLaughlin, and R. Surman, Phys. Rev. C **85**, 045801 (2012).
[11] B. Pfeiffer *et al.*, in *Proceedings of the Specialists' Meeting on Delayed Neutron Properties* (Birmingham University, Birmingham, England, 1986), p. 75.
[12] S. Nishimura *et al.*, Phys. Rev. Lett. **106**, 052502 (2011).
[13] G. Lorusso *et al.*, Phys. Rev. Lett. **114**, 192501 (2015).
[14] G. Lhersonneau *et al.*, Z. Phys. A **351**, 357 (1995).
[15] J. Dilling, R. Kruecken, and G. Ball, Hyperfine Interact. **225**, 1 (2014).
[16] A. B. Garnsworthy and P. E. Garrett, Hyperfine Interact. **225**, 121 (2014).
[17] G. Lhersonneau *et al.*, Z. Phys. A **352**, 293 (1995).
[18] E. A. McCutchan, N. V. Zamfir, and R. F. Casten, Phys. Rev. C **69**, 064306 (2004).
[19] G. Lhersonneau, P. Pfeiffer, R. Capote, J. M. Quesada, H. Gabelmann, and K. L. Kratz (ISOLDE Collaboration), Phys. Rev. C **65**, 024318 (2002).
[20] P. Möller, J. R. Nix, and K.-L. Kratz, At. Data Nucl. Data Tables **66**, 131 (1997).
[21] C. J. Gallagher and S. A. Moszkowski, Phys. Rev. **111**, 1282 (1958).
[22] T. Kibédi *et al.*, Nucl. Instrum. Methods Phys. Res., Sect. A **589**, 202 (2008).
[23] *Evaluated Nuclear Structure Data File (ensdf)*, http://www.nndc.bnl.gov/ensdf.
[24] E. A. McCutchan, A. A. Sonzogni, T. D. Johnson, D. Abriola, M. Birch, and B. Singh, Phys. Rev. C **86**, 041305(R) (2012).
[25] V. V. Simon, T. Brunner, U. Chowdhury, B. Eberhardt, S. Ettenauer, A. T. Gallant, E. Mane, M. C. Simon, P. Delheij, M. R. Pearson, G. Audi, G. Gwinner, D. Lunney, H. Schatz, and J. Dilling, Phys. Rev. C **85**, 064308 (2012).
[26] L. Mathieu *et al.*, AIP Conf. Proc. **1175**, 285 (2009).
[27] K.-L. Kratz and G. Herrmann, Z. Phys. **263**, 435 (1973).
[28] B. Pfeiffer, K.-L. Kratz, and P. Möller, Prog. Nucl. Energy **41**, 39 (2002).